Properties of Ganglioside G_{M1} in Phosphatidylcholine Bilayer Membranes

Robert A. Reed and G. Graham Shipley
Departments of Biophysics and Biochemistry, Boston University School of Medicine, Center for Advanced Biomedical Research, Boston, Massachusetts 02118 USA

ABSTRACT Gangliosides have been shown to function as cell surface receptors, as well as participating in cell growth, differentiation, and transformation. In spite of their multiple biological functions, relatively little is known about their structure and physical properties in membrane systems. The thermotropic and structural properties of ganglioside G_{M1} alone and in a binary system with 1,2-dipalmitoyl phosphatidylcholine (DPPC) have been investigated by differential scanning calorimetry (DSC) and x-ray diffraction. By DSC hydrated G_{M1} undergoes a broad endothermic transition T_M = 26°C (ΔH = 1.7 kcal/mol G_{M1}). X-ray diffraction below (−2°C) and above (51°C) this transition indicates a micellar structure with changes occurring only in the wide angle region of the diffraction pattern (relatively sharp reflection at 1/4.12 $Å^{-1}$ at −2°C; more diffuse reflection at 1/4.41 $Å^{-1}$ at 51°C). In hydrated binary mixtures with DPPC, incorporation of G_{M1} (0–30 mol %; zone 1) decreases the enthalpy of the DPPC pretransition at low molar compositions while increasing the T_M of both the pre- and main transitions (limiting values, 39 and 44°C, respectively). X-ray diffraction studies indicate the presence of a single bilayer gel phase in zone 1 that can undergo chain melting to an L_α bilayer phase. A detailed hydration study of G_{M1} (5.7 mol %)/DPPC indicated a conversion of the DPPC bilayer gel phase to an infinite swelling system in zone 1 due to the presence of the negatively charged sialic acid moiety of G_{M1}. At 30–61 mol % G_{M1} (zone 2), two calorimetric transitions are observed at 44 and 47°C, suggesting the presence of two phases. The lower transition reflects the bilayer gel → L_α transition (zone 1), whereas the upper transition appears to be a consequence of the formation of a nonbilayer, micellar or hexagonal phase, although the structure of this phase has not been defined by x-ray diffraction. At >61 mol % G_{M1} (zone 3) the calorimetric and phase behavior is dominated by the micelle-forming properties of G_{M1}; the presence of mixed G_{M1}/DPPC micellar phases is predicted.

INTRODUCTION

Gangliosides are complex glycosphingolipids composed of a ceramide backbone that anchors them within the membrane, an oligosaccharide polar group containing neutral sugars (i.e., glucose, galactose, *N*-acetyl-galactosamine, etc.) and a negatively charged sugar, sialic acid. Generally, gangliosides are found at their highest concentrations in the brain, localized in nerve endings and synaptic membranes (Norton and Podulso, 1971). However, gangliosides are also found in most cell types and were originally thought to reside exclusively in the extracellular monolayer of the cell membrane (Fishman and Brady, 1976). More recent studies argue that some gangliosides are located "internally" where they are involved in binding, e.g., to the cytoskeleton (Gillard et al., 1991) and, perhaps, to cytoplasmic proteins such as calmodulin (Higashi et al., 1992). In model membrane systems, e.g., unilamellar vesicles, it has been shown that gangliosides distribute between the two monolayer surfaces (Cestaro et al., 1980; Maggio et al., 1988).

Gangliosides are thought to be involved in many cellular functions including 1) cellular transformation; 2) cell-cell recognition; 3) interactions with extracellular matrix proteins; 4) modulation of cell growth; 5) affectors of cell morphology; 6) receptors for hormones such as interferon, interleukin 2, thyrotropin, and serotonin; 7) receptors for viruses including influenza virus and Sendai virus; and 8) receptors for toxins including cholera, tetanus, and botulinum toxins. In spite of this plethora of cell-associated functions mediated by gangliosides in the plasma membrane (for reviews, see Hakomori, 1981, 1990; Zeller and Marchase, 1992; Hakomori and Igarashi, 1993; Fishman et al., 1993; Fredman, 1993; Tettamanti and Riboni, 1993) and some understanding of their intracellular trafficking (Hoekstra and Kok, 1992), relatively little is known about the structure and properties of gangliosides or their interaction with other membrane lipids. An added incentive comes from the recent description of detergent-resistant glycosphingolipid/cholesterol-rich domains in membranes, which appear to sequester specific membrane proteins (Brown and Rose, 1992; Schnitzer et al., 1995; for a discussion, see Parton and Simons, 1995). Such structures include the caveolin-containing membrane invaginations, caveolae, and perhaps other membrane domains. The involvement of gangliosides, including ganglioside G_{M1} (G_{M1}), in such functional domains suggests that an improved description of the interaction of G_{M1} with other membrane lipid components (phospholipids, cholesterol, etc.) would be valuable.

Early physical studies showed that mixed gangliosides form micelles in dilute aqueous solutions above the critical micellar concentration, 0.02g/100 ml) with an average micellar weight between 250,000 and 450,000 Da (Gammack, 1963). Differential scanning calorimetry (DSC) and x-ray diffraction studies showed that bovine brain gangliosides at

Received for publication 3 May 1995 and in final form 3 November 1995.
Address reprint requests to G. Graham Shipley, Department of Biophysics, Boston University School of Medicine, 80 E. Concord St., Boston, MA 02118-2394. Tel.: 617-638-4009; Fax: 617-638-4041; E-mail: shipley@med-biophi.bu.edu.

0006-3495/96/03/1363/10 $2.00

lower hydrations exhibited a broad thermal transition and formed a cylindrical hexagonal (H_I) phase, rather than a bilayer phase (Curatolo et al., 1977). Aqueous dispersions of mixed gangliosides and egg yolk phosphatidylcholine (EYPC) were examined using electron microscopy; lamellar structures were observed at low ganglioside concentrations (<30%), spherical micelles at high ganglioside concentrations (>80%) and cylindrical structures at 45–48% ganglioside-EYPC (Hill and Lester, 1972). It was suggested that the cylindrical structure represented an intermediate in the conversion from a lamellar phase to a micellar phase.

The separation of ganglioside subclasses differing in their sialic acid content (monosialoganglioside G_{M1}, disialoganglioside G_{D1a}, and trisialoganglioside G_{T1b}, etc.) has led to studies of the properties of specific gangliosides. For example, using ferritin-conjugated cholera toxin to label G_{M1}, and freeze-etch microscopy to monitor the membrane distribution of the ganglioside in 1,2-dimyristoyl PC (DMPC), it was concluded that G_{M1} (1–20 mol % G_{M1}) was randomly distributed in the DMPC gel phase, and therefore not phase-separated into domains (Thompson et al., 1985). The thermotropic behavior of G_{M1} alone and in mixtures with 1,2-dipalmitoyl PC (DPPC) was studied using high sensitivity scanning calorimetry (Maggio et al., 1985a,b). As the headgroup complexity increased, both the temperature and enthalpy associated with the endothermic "micellar" transition decreased. Subfractions of G_{M1} containing homogeneous sphingosine base and amide-linked fatty acids (90–95% homogeneous) in mixtures with either DPPC or 1,2-distearoyl PC were examined using high sensitivity microcalorimetry (Masserini and Freire, 1986). No cooperative phase transition was observed for the homogeneous G_{M1} subfractions; however, the "heterogeneous" G_{M1} gave a single endothermic transition from 12 to 33°C. Masserini and Freire (1986) suggest that the transition observed for heterogeneous G_{M1} does not represent cooperative chain melting, but rather structural packing rearrangements associated with the heterogeneity in the hydrocarbon region.

Other studies of gangliosides have employed calorimetry (Bunow and Bunow, 1979; Sillerud et al., 1979; Hinz et al., 1981; Bach et al., 1982), nuclear magnetic resonance (Harris and Thornton, 1978; Koerner et al., 1983a,b; Scarsdale et al., 1990; Acquotti et al., 1990; Sabesan et al., 1984, 1991; Singh et al., 1992; Siebert et al., 1992), surface monolayers (Maggio et al., 1978a,b, 1980, 1981; Perillo et al., 1993), freeze-etch electron microscopy (Peters et al., 1984; Mehlhorn et al., 1986), and x-ray diffraction (McDaniel and McIntosh, 1986; McIntosh and Simon, 1994). Through such studies an improved picture of ganglioside properties and ganglioside-phospholipid interactions is beginning to emerge.

As part of our studies of 1) glycosphingolipid structure, properties and lipid interactions (Ruocco et al., 1981, 1983; Ruocco and Shipley, 1984, 1986; Reed and Shipley, 1987, 1988; Haas and Shipley, 1995) and 2) the interaction of cholera toxin with its membrane receptor, ganglioside G_{M1}, in membrane monolayer/bilayer model systems (Reed et al., 1987; Cabral-Lilly et al., 1994) and in crystals (Zhang et al., 1995a,b), we have begun to examine the interactions of gangliosides with phospholipids. Here, we describe x-ray diffraction and scanning calorimetry studies of G_{M1} alone and in a binary system with DPPC. Although the DSC studies cover the whole range of binary G_{M1}/DPPC compositions, the structural data focus more extensively on G_{M1} compositions <30 mol % where bilayer structures are formed. The latter should provide information relevant to the organization of gangliosides in cell membranes and membrane domains. At higher G_{M1} contents, one would expect the micelle-forming G_{M1} to exert its detergent properties forming lipid structures of high curvature, i.e., rods/hexagonal phases, spherical mixed micelles, etc. We have collected x-ray diffraction data at higher mol % G_{M1}; however, their interpretation in terms of specific phases and mixtures of phases is not straightforward.

MATERIALS AND METHODS

Samples

Bovine brain gangliosides were extracted according to the procedure of Svennerholm and Fredman (1980), and the separation of the gangliosides into mono-, di-, and trisialo gangliosides (G_{M1}, G_{D1a}, and G_{T1b}) was accomplished using the procedure of Myers et al. (1984); see also Reed et al. (1987). DPPC was purchased from Avanti Polar Lipids, Inc. (Birmingham, AL) and gave a single spot by thin-layer chromatography in the solvent system chloroform/methanol/water (65:25:4, v/v). When multiple spots were observed, DPPC was purified by passing it over an Iatrobead column 8060 (Iatron Laboratories, Tokyo, Japan) and eluting with a stepwide gradient of chloroform/methanol (100:0 up to 50:50, v/v). The fractions corresponding to chromatographically pure DPPC were evaporated to dryness, lyophilized, and used without further purification.

Calorimetry

For experiments performed on the Perkin-Elmer DSC-2C (Norwalk, CT), hydrated samples were prepared by weighing either DPPC or G_{M1} into a stainless steel pan, followed by the introduction of distilled water with a microsyringe to make a 70 wt % water dispersion; in some experiments lower water contents were used. The pans were hermetically sealed and cycled above and below the transition temperature(s) of the lipid to ensure equilibration. G_{M1}/DPPC binary systems were prepared by weighing both lipids into a stainless steel pan. The mixture was dissolved in 2:1 (v/v) chloroform:methanol, followed by solvent evaporation under a stream of N_2. This procedure was repeated several times to ensure proper mixing. The sample was then dried, lyophilized, and reweighed to check for sample loss. Sample hydration and equilibration were carried out as described above. Heating and cooling rates ranged from 1.25 to 5 °C/min. Transition temperatures and enthalpies were computed using the Perkin-Elmer DSC-2C analysis software after calibration with a known gallium standard.

For experiments performed on the Microcal (Northampton, MA) MC2 scanning calorimeter, G_{M1} was weighed into a small vial, hydrated with buffer (0.05 M phosphate buffer, pH 7), degassed for at least 30 min, injected into the sample cell and run against buffer. Scanning rates were usually 1.0–1.5°C/min.

X-ray diffraction

Hydrated samples were prepared by weighing DPPC or G_{M1} into thin-walled (internal diameter = 1 mm) glass capillaries (Charles Supper, Natick, MA). Distilled water was added with a microsyringe to make the

desired wt % water dispersions. For equilibration, the sample tubes were centrifuged at room temperature, the capillary flame sealed, and the sample centrifuged at least eight times through the capillary at a temperature above the phase transition of the lipid.

Binary G_{M1}/DPPC samples were prepared by weighing each lipid into a glass tube that had a constricted center. The mixture was dissolved in chloroform:methanol (1:1, v/v) and evaporated under a stream of nitrogen gas. The sample was lyophilized, reweighed, hydrated, and the glass tube flame-sealed. The sample was equilibrated by centrifuging through the constricted center at least 12 times, at a temperature above its calorimetric transition. After breaking open the glass tube, the sample was rapidly transferred to a thin-walled capillary tube and the capillary tube flame-sealed.

X-ray diffraction experiments were carried out with nickel-filtered CuK_α x-radiation (λ = 1.5418 Å) from an Elliot GX-6 rotating anode x-ray generator (Elliot Automation, Borehamwood, UK) and focused by a toroidal mirror camera. Samples were kept at constant temperature by a circulating ethylene glycol/water bath. The sample temperature was monitored continuously by a thermocouple adjacent to the sample. The diffraction patterns were recorded on Kodak No-screen x-ray film and the diffracted intensities measured using a Joyce-Loebl (Gateshead, UK) model IIICS scanning microdensitometer. For the hydration study, diffraction patterns were recorded using a multifocus x-ray generator (Jarrell-Ash Co., Waltham, MA) with CuK_α x-radiation focused and collimated using a Luzzati-Baro (E^{TS} Beaudouin, Paris, France) camera. Intensity data were collected by a linear position-sensitive detector (Tennelec, Oak Ridge, TN) and analyzed by a Tracor computer interfaced to the position-sensitive detector (Tracor Northern, Madison, WI) and processed as described in the Results section.

RESULTS

Ganglioside G_{M1}

DSC heating and cooling scans (5°C/min) of hydrated G_{M1} (70 wt % water) are shown in Fig. 1 *A*. Heating from −10°C produces a very broad endothermic transition (range, ~5–40°C) with a peak maximum at ~26°C. The enthalpy associated with this broad transition is 1.7 kcal/mol G_{M1}. Upon cooling, a broad exothermic transition is observed (T_m ~ 22°C; ΔH = −1.7 kcal/mol G_{M1}). These calorimetric heating and cooling scans are reproducible and confirm the essentially reversible behavior of this broad transition. The heating and cooling transitions are unchanged after long-term incubations at low temperature (data not shown). The behavior of a dilute solution of G_{M1} (5.80 mg/ml in phosphate buffer) recorded on a high sensitivity scanning calorimeter at 1.5°C/min is shown in Fig. 1 *B*. A broad endothermic transition is observed from 5 to 40°C (peak maximum 23.5°C ΔH = 1.7 kcal/mol G_{M1}, in good agreement with the data shown in Fig. 1 *A*.

X-ray diffraction techniques were used to investigate the structures of G_{M1} present at temperatures below and above the calorimetric transition. The diffraction pattern in Fig. 2 *A* is from a hydrated (70 wt % water) G_{M1} sample and was recorded at −2°C. Visually the sample appeared optically clear. The diffraction pattern shows two broad diffraction maxima in the low angle region and a single, fairly sharp reflection at 1/4.12 $Å^{-1}$ (Fig. 2 *A*, *arrow*) in the wide angle region. The strongest scattering in the low angle region is centered at d = 35.0 Å, with much weaker scattering at d = 12.8 Å. This optically isotropic solution of G_{M1} shows

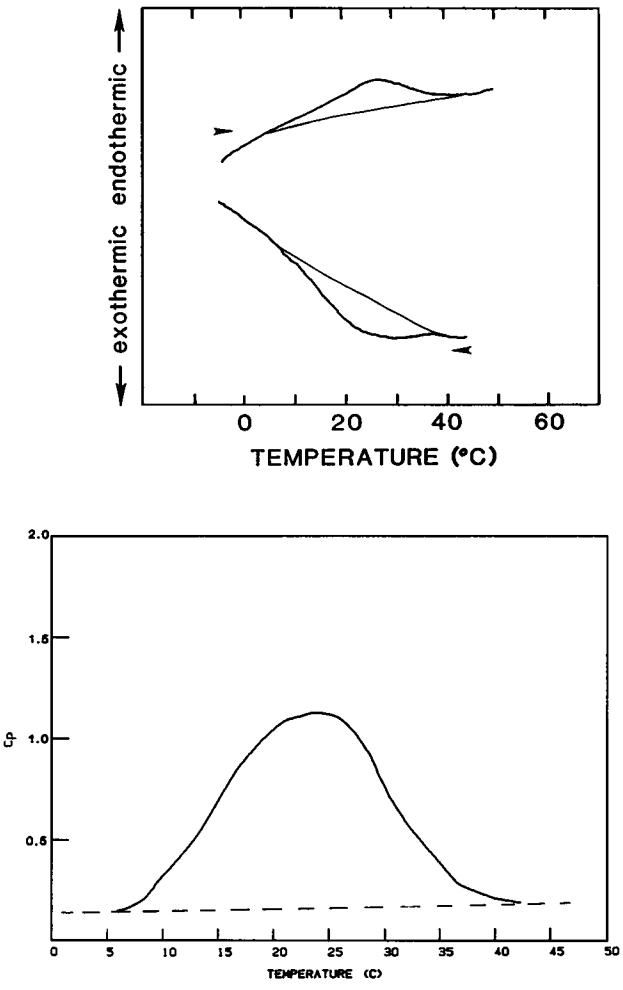

FIGURE 1 (*A*) DSC heating/cooling scans of hydrated (70 wt % H_2O) ganglioside G_{M1} recorded on the Perkin-Elmer DSC-2C scanning calorimeter; heating/cooling rate, 5°C/min; (*B*) DSC heating scan for hydrated (5.80 mg G_{M1}/ml phosphate buffer) ganglioside G_{M1} recorded on the Microcal MC2 scanning calorimeter; heating rate, 1.5°C/min).

continuous scattering as opposed to the sharp diffraction maxima from a multilamellar (or other ordered) lipid system. The diffraction pattern in Fig. 2 *B* was recorded at 51°C, a temperature above the broad transition maximum observed by DSC, and shows no changes in the low angle region compared with that observed at −2°C, i.e., two broad scattering maxima at approximately 35 and 13 Å. However, the reflection in the wide angle region has shifted to 1/4.41 $Å^{-1}$ (Fig. 2 *B*, *arrow*) and has broadened significantly. At this temperature, the sample remained optically clear.

G_{M1}/DPPC binary mixtures

The calorimetric behavior of hydrated (70 wt % water) G_{M1}/DPPC binary mixtures is shown in Fig. 3 (heating rate = 5°C/min). DPPC shows the characteristic $L_{\beta'} \rightarrow P_{\beta'}$ pretransition at 34.5°C (ΔH = 0.7 cal/g lipid) followed by the main chain-melting transition at 41.5°C (ΔH = 10.5 cal/g lipid). Addition of G_{M1} increases the T_m of both the

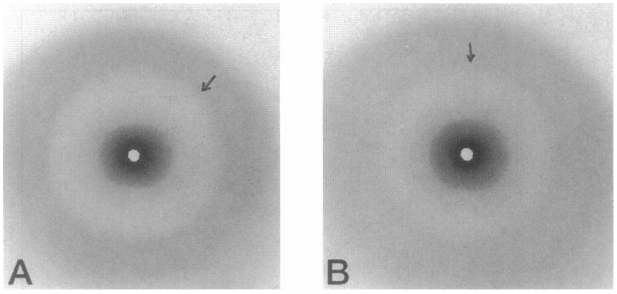

FIGURE 2 X-ray diffraction patterns of hydrated (70 wt % water) ganglioside G_{M1} at −2°C (*A*) and 51°C (*B*) recorded using toroidal optics; sample-film distance, 63.5 mm. Arrows indicate diffraction maxima at 1/4.12 $Å^{-1}$ (*A*) and 1/4.41 $Å^{-1}$ (*B*). The outermost broad maxima are due to scattering from water.

pretransition and the chain-melting transition; also, the chain-melting transition shows progressive broadening. At 17.8 mol % G_{M1}, the pretransition has increased in temperature to 39°C and has become a small shoulder on the edge of the main transition, whereas the chain-melting transition has broadened and increased in temperature to 43.7°C (ΔH = 10.2 cal/g lipid). At 28.7 mol % G_{M1}, the decreased cooperativity of this transition and the more pronounced high temperature shoulder suggest the onset of phase separation. At 38.7 mol % G_{M1}, two endothermic transitions occur at 43.8 and 46.7°C (combined enthalpy, 6.4 cal/g), clearly indicating phase separation. At 46.5 and 61.3 mol % G_{M1}, a significant decrease is observed in the enthalpy associated with the lower transition, essentially reaching 0 by 61.3 mol % G_{M1}. The enthalpy of the combined transition decreases to ΔH = 2.3 cal/g at 61.3 mol % G_{M1}, and a new low temperature endothermic transition has appeared at 19.0°C (ΔH = 0.4 cal/g). Increasing to 76.8 and 86.2 mol % G_{M1} leads to an increase in both the T_m and enthalpy of this low temperature transition and a decrease in the T_m and enthalpy of the higher transition. At 94.4 mol % G_{M1} a single broad transition (T_m = 26.9°C, ΔH = 1.5 cal/g) is observed, similar to that of pure G_{M1} shown in Fig. 1 *A* (T_m = 23°C (range 5–40°C; ΔH = 1.7 kcal/mol G_{M1}). The pattern of calorimetric changes observed with increasing G_{M1} content is summarized in Fig. 8.

X-ray diffraction patterns were recorded at different binary G_{M1}/DPPC compositions at a fixed hydration (70 wt % water) and, in some cases, at different temperatures. The presence of negatively charged G_{M1} molecules in DPPC bilayers (or other lipid phases) causes the system to hydrate and in the case of lamellar phases a large interbilayer aqueous layer results. This leads to lamellar stacking disorder, and the low angle reflections at this hydration are diffuse. The lamellar diffraction pattern of hydrated (70 wt % water) DPPC, bilayer periodicity d = 63.4 Å (h = 1–5) recorded at 20°C is shown in Fig. 4 *A*. The two wide angle reflections (1/4.2 $Å^{-1}$ and 1/4.1 $Å^{-1}$, *arrows*) are indicative of quasi-hexagonally packed chains which are tilted with respect to the bilayer normal. Diffraction patterns recorded at 26 and 46°C correspond to the rippled, gel phase ($P_{\beta'}$)

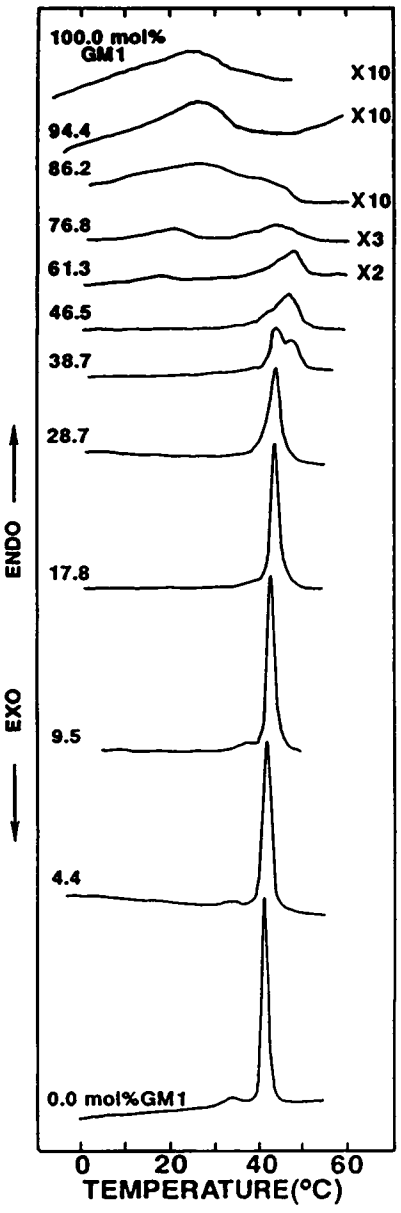

FIGURE 3 DSC heating scans of hydrated G_{M1}/DPPC binary mixtures recorded on the Perkin-Elmer DSC-2C scanning calorimeter; heating rate, 5°C/min. mol % G_{M1} is listed on the right.

and melted chain, liquid crystalline (L_α) phase, respectively (data not shown). At 20°C, the presence of 16.3 mol % G_{M1} results in a large increase in bilayer periodicity, d = 125 Å (h = 1–4, diffuse), and a single strong wide angle reflection at 1/4.17 $Å^{-1}$ (*arrow*) is indicative of a highly hydrated bilayer gel phase but with reduced chain tilt (Fig. 4 *B*). At 57°C the bilayer periodicity is reduced to d = 116 Å and a diffuse wide-angle reflection at $1/4.6^{-1}$ is observed (data not shown). The diffraction pattern for DPPC containing 36.5 mol % G_{M1} is also indicative of a highly hydrated gel phase (d = 132 Å; 1/4.21 $Å^{-1}$, *arrow*) at 20°C (Fig. 4 *C*); at 55°C a small reduction in bilayer periodicity (d = 129 Å) accompanies chain melting (data not shown). A further

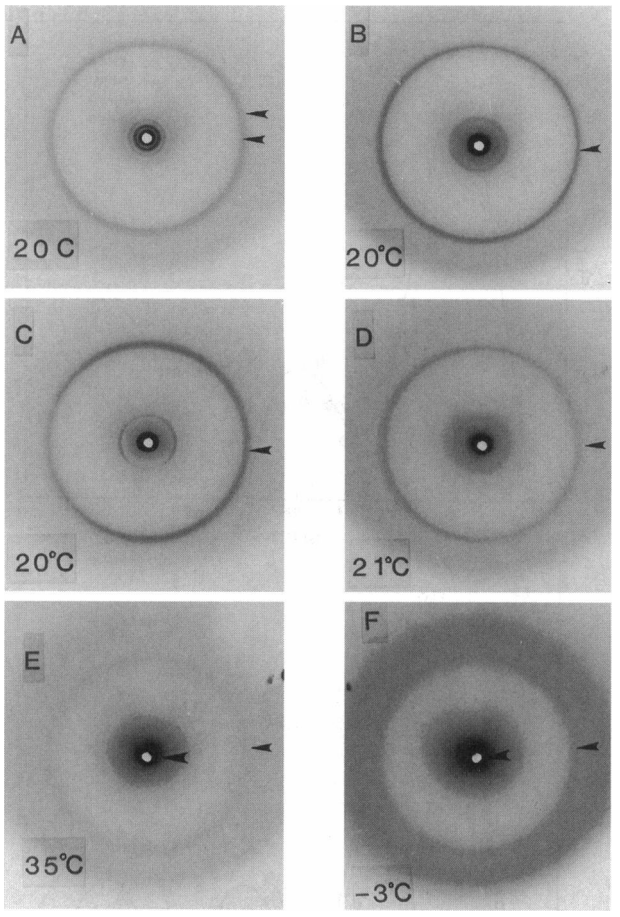

FIGURE 4 X-ray diffraction patterns of hydrated (70 wt % water) binary mixtures of G_{M1}/DPPC. (*A*) 100 mol % DPPC, 20°C; (*B*) 16.3 mol % G_{M1}, 20°C; (*C*) 36.5 mol % G_{M1}, 20°C; (*D*) 57.9 mol % G_{M1}, 21°C; (*E*) 78.3 mol % G_{M1}, 35°C; 100 mol % G_{M1}, −3°C.

increase to 57.9 mol % G_{M1} (i.e., well beyond the phase boundary) produces the diffraction pattern at 21°C shown in Fig. 4 *D*. While the hydrated bilayer gel phase appears to be present (d = 127 Å; 1/4.27 $Å^{-1}$, *arrow*), a more diffuse reflection at 60 Å suggests the presence of an additional phase. At 51°C a complex diffraction pattern is observed with two of the low angle reflections indexing to a bilayer periodicity 123 Å (data not shown). For 78.3 mol % G_{M1} the diffraction pattern (Fig. 4 *E*) recorded at 35°C between the two calorimetrically observed transitions (see Figs. 3 and 8) resembles that of pure G_{M1} (Fig. 4 *F*; also, see Fig. 2 *A*) with strong, broad scattering centered at 60 Å (*inner arrow*), and weaker scattering at 20 and 14 Å. At 51°C, two diffuse low angle reflections at ~60 and ~13 Å are observed together with a diffuse wide angle reflection at 1/4.5 $Å^{-1}$ (data not shown). As described previously, hydrated G_{M1} alone at −3°C shows two broad scattering maxima at 36 (*inner arrow*) and 13 Å, as well as a wide angle reflection at 1/4.13 $Å^{-1}$ (*outer arrow*) (Fig. 4 *F*; also, see Fig. 2 *A*). Above the broad transition exhibited by hydrated G_{M1}, the diffraction pattern shown in Fig. 2 *B* is observed (scattering maxima, 35 and 13 Å; wide angle reflection, 1/4.41 $Å^{-1}$).

X-ray diffraction patterns were also recorded at −4°C (i.e., below the first broad transition; see Figs. 3 and 7) for G_{M1}/DPPC binary mixtures containing 57.9 and 78.3 mol % G_{M1}. However, only minor differences are observed compared with those recorded at 20 and 35°C, respectively.

G_{M1}(5.7 mol %)-DPPC binary mixture

To define further the effects of low molar contents of G_{M1} on the structure of DPPC bilayers, an x-ray diffraction study was performed as a function of hydration. Diffraction patterns from a binary mixture, 5.7 mol % G_{M1}/DPPC, containing 20.0, 29.8, 42.1, 50.4, and 61.0 wt % water were recorded at 22°C, i.e., below the pre- and chain-melting transitions of DPPC, in the gel phase. In all cases, the wide angle region displays two reflections, a strong, sharp reflection at 1/4.2 $Å^{-1}$ and a much weaker reflection at ~1/4.1 $Å^{-1}$. The presence of these two reflections confirms that at 5.7 mol % G_{M1} and 20–61% water, the bilayer remains as a gel phase with pseudo-hexagonally packed, tilted hydrocarbon chains. In the low angle region lamellar reflections are observed in all cases and, as the hydration increases, changes are observed in both the positions and intensities of the lamellar reflections (data not shown). A plot of the bilayer periodicity (d) as a function of hydration (wt % water) is shown in Fig. 5 *A* and compared with that of hydrated DPPC alone. For the G_{M1}/DPPC system, the repeat distance, d, increases continuously with increased water content, at least up to 61 wt % water. A broadening of the low angle reflections is observed at higher hydrations because of multibilayer stacking disorders (Gulik-Krzywicki et al., 1969). This continuous swelling behavior of G_{M1}/DPPC contrasts with the limited hydration (hydration maximum; 30 wt % water) exhibited by DPPC alone (see Fig. 5 *A*). Plotting the bilayer repeat distance, d, as a function of $1 - C/C$, where C is the concentration of lipid (weight fraction), results in a linear dependence for hydrated G_{M1}/DPPC as shown in Fig. 5 *B*. This indicates that the

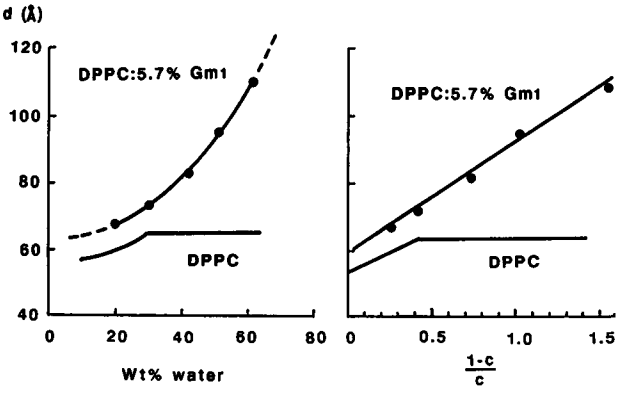

FIGURE 5 X-ray diffraction data for DPPC and a G_{M1}(5.7 mol %)/DPPC binary mixture at 23°C. (*A*) Bilayer periodicity, d(Å), as a function of wt % H_2O; (*B*) bilayer periodicity, d(Å), as a function of $1 - C/C$ (C = total lipid concentration).

G_{M1}/DPPC bilayer structure, specifically its thickness, is not undergoing significant changes as the hydration state is changed. Extrapolating $1 - C/C$ to 0 yields the constant lipid bilayer thickness (d_1 = 60 Å) for G_{M1}/DPPC in the presence of water, compared with a value of 54 Å for DPPC (see Fig. 5 *B*).

From the observed intensity data ($I(s)$obs), scaled structure amplitudes, $F(s)$, were calculated. The observed intensities were corrected for the Lorentz factor ($I(s) = s^2.I(s)$obs), and each hydration set was normalized with respect to each other using the procedure described by Worthington and Blaurock (1969), i.e.,

$$2/d\sum s^2.I(s) = \text{constant}$$

The corresponding scaled, normalized structure amplitudes $F(s)$ plotted as a function of $s = (2 \sin \theta/\lambda)$ yield the continuous structure amplitude curve shown in Fig. 6 *A*. The continuous curve describes the Fourier transform of a single bilayer and allows the positions in reciprocal space where the Fourier transform changes sign to be determined. This provides a method for establishing the phases of the set of structure amplitudes corresponding to each hydration. After calculating the zero-order amplitude $F(0)$ according to the method described by King (1971) and King and Worthington (1971), the continuous transforms were calculated using the Shannon sampling theory (Shannon, 1949; Sayre, 1952; King and Worthington, 1971) and are shown in Fig. 6 *B*. The five individual curves represent the five data sets obtained from the swelling study; they show quite clearly where the first three zeros in the amplitude curve occur and lead to an unambiguous phase assignment for each set of structure amplitudes.

Using the phased amplitudes, one-dimensional electron density profiles of hydrated G_{M1}(5.7 mol %)/DPPC bilayers have been calculated by Fourier transformation. Fig. 7 shows the five electron density profiles as a function of hydration. A characteristic bilayer profile is observed in each case; the two peaks in electron density are due primarily to the electron-dense phosphate groups in the DPPC headgroup, while the trough at $X = 0$ Å corresponds to the inefficient hydrocarbon chain packing at the bilayer center. The distance between the two electron-rich peaks gives the phosphate-phosphate separation distance across the bilayer (d_{p-p}), another measure of the bilayer thickness (see Fig. 7, *top*). The region of intermediate electron density is due to the hydration layer between adjacent bilayers and d_w, a measure of the thickness of the hydration layer can be calculated (see Fig. 7, *top*). For all five hydrations of G_{M1}/DPPC, d_{p-p} is constant at 44 Å; in contrast, the thickness of the hydration layer, d_w, predictably increases as a function of hydration. Thus, d_w increases from 23.5 Å at 20.0 wt % water to 65.0 Å at 61.0 wt % water. The profiles are similar in the bilayer region except for a loss of detail at the higher hydrations, probably because of resolution effects and stacking disorder. While peaks are observed in the hydration layer, it is not appropriate at this stage to attribute them to specific structural details such as the location on the oligosaccharide head groups of G_{M1} at the bilayer surface (see Discussion).

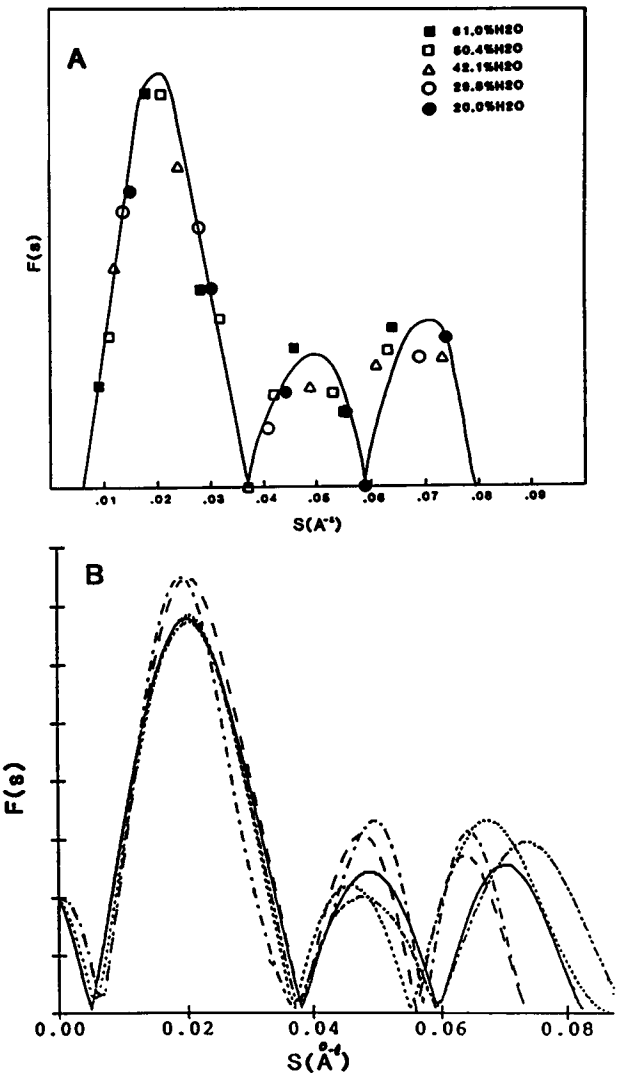

FIGURE 6 X-ray diffraction data for a G_{M1}(5.7 mol %)/DPPC binary mixture at 23°C. (*A*) Corrected structure amplitudes, $F(s)$, where $s = 2 \sin \theta/\lambda$; (●) 20.0, (○) 29.8, (△) 42.1, (□) 50.4, and (■) 61.0 wt % water. (*B*) Continuous amplitude curves, $F(s)$, for each hydration calculated using the sampling theorem (Shannon, 1949).

DISCUSSION

The structure and thermotropic properties of hydrated binary mixtures of gangliosides G_{M1} and DPPC have been investigated using calorimetry and x-ray diffraction. Previously, the properties of bovine brain gangliosides (a heterogenous mixture of mono-, di-, and trisialogangliosides) were investigated using polarizing light microscopy, calorimetry, and x-ray diffraction (Curatolo et al., 1977). Two endothermic transitions centered at 30 and 49°C were observed. An hexagonal (HI) phase was observed over the

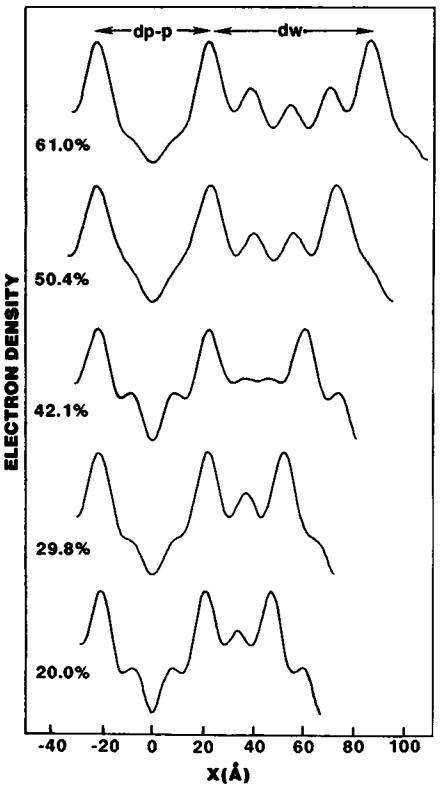

FIGURE 7 Bilayer electron density profiles, $\rho(X)$, for a G_{M1}(5.7 mol %)/DPPC binary mixture at 20.0, 29.8, 42.1, 50.4, and 61.0 wt % water at 23°C. d_{p-p}, lipid bilayer thickness; d_w, interbilayer water thickness.

hydration range 18–50 wt % water. Below the 30°C transition a single, diffuse reflection was observed in the wide angle region, centered at 1/4.2 $Å^{-1}$, whereas above the 49°C transition a diffuse reflection was centered at 1/4.5 $Å^{-1}$. As the hydrated ganglioside was heated through the 30°C transition the reflection at 1/4.2 $Å^{-1}$ remained unchanged, but then gradually shifted to 1/4.5 $Å^{-1}$ on heating through the 49°C transition. A subsequent calorimetric study of hydrated bovine brain gangliosides in phosphate buffer also observed two broad, overlapping endothermic transitions at 27 and 46°C (Bunow and Bunow, 1979); these authors also observed two broad, overlapping transitions at 26 and 43°C for G_{M1} in phosphate buffer. Using ethylene glycol/Tris as buffer, Bach et al. (1982) also demonstrated two broad transitions for G_{M1} at 20 and 40°C.

Next, a calorimetric study of various hydrated glycosphingolipids including gangliosides demonstrated a single, broad endothermic transition for G_{M1} with a maximum at 19.3°C, ΔH = 0.8 kcal/mol (Maggio et al., 1985a). Surprisingly, a study of hydrated G_{M1} with homogenous fatty acid and sphingosine chain length, produced no calorimetric transitions, while G_{M1} with a heterogeneous sphingosine base composition gave a single endothermic transition (Masserini and Freire, 1986). The authors suggest that the G_{M1} transition was related to structural rearrangements in ganglioside micelles related to the heterogeneous hydrocarbon chain length.

The calorimetric behavior observed in the present study of hydrated G_{M1}, is in close agreement with those of Maggio et al. (1985a) and Masserini and Freire (1986). On heating, a single, broad endothermic transition is observed, centered at 23–25°C, ΔH = 1.7 kcal/mol (Fig. 1). The combination of the optical properties and the x-ray diffraction data indicate that at the hydrations used here (70 wt % water) micellar phases exist both below and above the phase transition. The two broad x-ray maxima at 35 and 13 Å are characteristic of the scattering of micelles and apparently the two micellar phases differ only in the packing arrangements of the hydrocarbon chains in the micelle interior. The relatively sharp reflection at 1/4.12 $Å^{-1}$ below the endothermic transition is indicative of more ordered hydrocarbon chain packing, while the broader reflection centered at 1/4.4 $Å^{-1}$ is typical of less ordered, fluid hydrocarbon chains in bilayer, hexagonal, cubic, and micellar lipid phases. Thus, the broad calorimetric transition of G_{M1} appears to be due to an order-disorder transition involving the hydrocarbon chains in the core of the micelle. However, at present, neither the more ordered packing arrangement of the two hydrocarbon chains (sphingosine and *N*-acyl) of G_{M1} in the micelle center nor the mechanism by which hydrocarbon chain order-disorder transitions could occur in micelles is clear. The presence of a single endothermic transition observed for G_{M1} in the more recent studies, as opposed to multiple transitions observed previously, is probably a result of improvements in methods of isolation and purification of gangliosides.

The effect of G_{M1} on the structure and thermotropic properties of hydrated DPPC bilayers was also investigated. A preliminary temperature-composition phase diagram based on the DSC (Fig. 3) and x-ray diffraction (Figures 4–7) data is shown in Fig. 8. The addition of up to to 9.5 mol % G_{M1} has little effect on the chain-melting transition of DPPC at ~42°C, other than a slight broadening (Fig. 3). However, G_{M1} does influence the pretransition, increasing the T_m and decreasing the enthalpy. With increasing G_{M1}, the pretransition associated with DPPC broadens, increases in T_m, overlaps with the chain-melting transition, and is no longer observed at 28.7 mol % G_{M1}. The maximum incorporation of G_{M1} into DPPC bilayers is reached at ~30 mol % G_{M1} as indicated by the appearance of a high-temperature shoulder on the chain-melting transition. Thus, in this region of the phase diagram (zone 1), a single DPPC-rich bilayer phase capable of incorporating up to ~30 mol % G_{M1} is present and increasing G_{M1} content results in a small increase in the chain melting transition of DPPC. The x-ray diffraction data (Figs. 4, *A* and *B*, and 5, *A* and *B*) show that in this compositional range (<30 mol % G_{M1}) G_{M1} is incorporated into the DPPC bilayer where it induces both interbilayer hydration (bilayer periodicity, 125–130 Å) and eventually, in the gel phase, relaxation of chain tilt. These mixed G_{M1}/DPPC bilayers undergo chain melting to an L_α bilayer phase while retaining the interbilayer water.

Between 30 and 60 mol % G_{M1} (zone 2), a separate high temperature peak is clearly present (Fig. 3). The x-ray

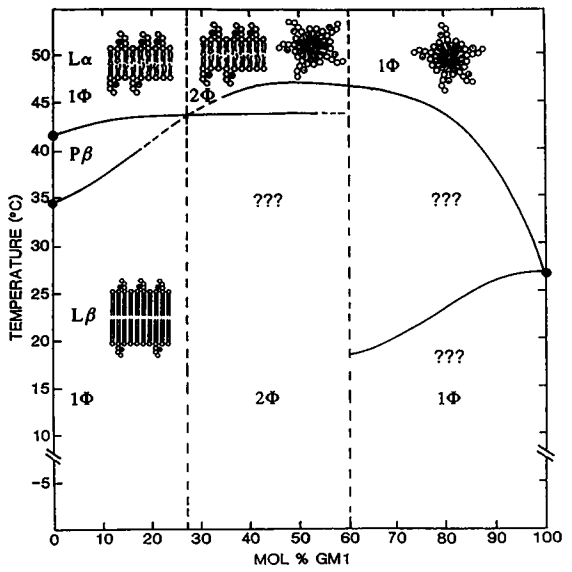

FIGURE 8 Partial temperature-composition phase diagram of the binary system, G_{M1}/DPPC, at 70 wt % hydration.

diffraction data show that at 36.5 mol % G_{M1} the highly hydrated bilayer phase which can undergo chain melting (see above) is still present, but the data do not provide evidence for a second coexisting phase. At 57.9 mol % G_{M1} the diffraction data do suggest the presence of two coexisting phases, including the hydrated bilayer gel phase (at least, at 20°C; see Fig. 4 *D*). However, the large degree of bilayer swelling induced by the anionic, charged G_{M1} leads to complications when interpreting the diffraction patterns. Unequivocal identification of coexisting phases in this region of the phase diagram is difficult, although it seems probable that the second higher melting phase formed at >30 mol % G_{M1} has either a micellar or cylindrical structure (see sketch in Fig. 8). Thus addition of G_{M1} over the range 30–60 mol % leads to the progressive disappearance of the lower temperature chain-melting transition as, presumably, the bilayer→"micelle" conversion continues; at ~60 mol % G_{M1} this transition is no longer present. Thus, in this central region (zone 2), 30–60 mol % G_{M1}, two phases coexist: the bilayer phase with maximally (30 mol %) incorporated G_{M1} (phase transition, 43°C) plus a micellar/cylindrical phase (phase transition, 46°C). Increasing the G_{M1} content progressively converts the bilayer phase to the mixed G_{M1}/DPPC micellar or cylindrical phase.

At >60 mol % G_{M1} the remaining broad transition at ~45°C is accompanied by the low temperature transition at 19°C (Fig. 3). Addition of G_{M1} in this zone leads to the progressive overlap and merging of these two transitions eventually to yield calorimetric behavior similar to that of pure G_{M1} (see Fig. 3). X-ray diffraction data recorded at 78.3 mol % G_{M1} showed two broad scattering maxima centered at ~60 and 14 Å in the low angle region, consistent with the presence of a micellar phase both between and above the two calorimetric transitions observed in this region (zone 3) of the phase diagram. However, there is a difference in the location of the first scattering maximum (~60 Å) compared with the micellar phase of pure G_{M1} (~36 Å). Perhaps this is due to the G_{M1}/DPPC mixed micelle retaining some bilayer/discoidal structural characteristics which differentiate it from a more symmetrically shaped G_{M1} micelle.

Our calorimetric results are in good agreement with two previous calorimetric studies of the binary G_{M1}/DPPC system. Sillerud et al. (1979) concluded that the maximum amount of G_{M1} that could be incorporated into DPPC bilayers was about 25 mol %; based on turbidity studies, these authors suggested that a mixed bilayer/micellar phase was present from 30 to 54 mol % G_{M1}, with only the mixed micellar phase existing at higher G_{M1} concentrations (>54 mol %). Using high sensitivity calorimetry, Maggio et al. (1985b) studied binary ganglioside-DPPC systems. Although the data for the G_{M1}-DPPC system were not presented, the authors state that qualitatively similar behavior was observed for both the G_{M3}/DPPC and G_{M1}/DPPC binary systems. For G_{M1}/DPPC, we observe behavior qualitatively similar to that shown by Maggio et al. (1985b) for the G_{M3}/DPPC system (and, by inference, the G_{M1}/DPPC system) where the G_{M3}/DPPC bilayer chain-melting transition was no longer observed at ~60 mol % G_{M3}.

We have also focused on the structure of the DPPC bilayer system containing low concentrations of G_{M1}. At 5.7 mol % G_{M1}, no major change in the calorimetric behavior is observed compared with pure DPPC, i.e., the pre- and chain-melting transitions are present. However, the x-ray diffraction experiments as a function of hydration show clearly that major changes occur with respect to the degree of hydration between the stacked, lamellar bilayers (Figures 5–7). The swelling phenomenon observed is not unexpected, since an anionic, charged lipid (G_{M1}) has been incorporated into the uncharged DPPC bilayers. The bilayer surfaces become negatively charged and, in the absence of excess counterion, will undergo charge-mediated electrostatic repulsion and continuous bilayer swelling is observed (Fig. 5). Based on the electron density profiles, the interbilayer hydration layer increases from 23.5 Å at 20 wt % water to a value of 65 Å at 61.0% water. However, the structure of the bilayer is essentially unchanged during this swelling as indicated both by the linearity of the d versus $1 - C/C$ plot (Fig. 5 *B*) and by the invariance of the bilayer thickness (d_{p-p} = 44 Å) from the electron density profiles (Fig. 7). The lipid bilayer thickness, d_l, was calculated to be 60 Å (Fig. 5 *B*), 16 Å greater than the d_{p-p} observed in the electron density profiles (Fig. 7). However, d_l is a measure of the "entire" lipid bilayer thickness and includes a contribution from the oligosaccharide moiety of G_{M1}, whereas d_{p-p} reflects the distance between the electron dense phosphate groups of the DPPC headgroup. The electron density profiles of DPPC-G_{M1} (Fig. 7) are similar to those observed for the G_{M1}/EYPC or G_{M1}/1-palmitoyl, 2-oleoyl PC (POPC) systems (McIntosh and Simon, 1994; McDaniel and McIntosh, 1986)), although they report on gel phase (d_{p-p} = 44 Å) and fluid phase (d_{p-p} = 40 Å) bilayers, respectively.

The wide angle diffraction patterns suggest a gel phase in which the hydrocarbon chains are hexagonally packed (1/4.2 $Å^{-1}$) and tilted (1/4.1 $Å^{-1}$). The observed bilayer thickness of 44 Å for the G_{M1}/DPPC system is in good agreement with previous studies of pure DPPC bilayers (Torbet and Wilkins, 1976; McIntosh and Simon, 1986). Thus, adding 5.7 mol % G_{M1} to DPPC bilayers has little effect on the preexisting DPPC bilayer structure. Apparently at low concentrations the G_{M1} can substitute for DPPC quite well in the DPPC lattice. However, the presence of the negatively charged sialic acid moiety of the G_{M1} oligosaccharide at the bilayer surface (even at a low molar concentration, 5.7 mol %) is sufficient to produce the charge repulsion effect responsible for continuous interbilayer hydration. Similar effects of simple charged amphiphiles on the hydration behavior of PC bilayers have been reported by Gulik-Krzywicki et al. (1969).

A structural study of G_{M1} in POPC was previously carried out using x-ray diffraction (McDaniel and McIntosh, 1986). This study was concerned with localizing the G_{M1} headgroup relative to the PC headgroup. Europium-labeled and unlabeled G_{M1} was incorporated into POPC bilayers and, as in our studies (see above), the swelling behavior was utilized for phasing purposes. The resulting electron density difference profile and modeling studies indicate that the heavy atom europium-carboxylate/sialic acid site is located in the interbilayer space, 10 Å from the center of the PC headgroup. This, in turn, suggests a fully extended G_{M1} oligosaccharide headgroup projecting perpendicular to the bilayer plane. However, even at 30 mol % G_{M1}, no electron density attributable to an unlabeled G_{M1} headgroup was observed in the profiles (McDaniel and McIntosh, 1986). Thus, while the electron density profiles shown in Fig. 7 contain small peaks in the interbilayer region, at this stage it is not possible to attribute these to the oligosaccharide moiety of G_{M1}. In a more recent study, McIntosh and Simon (1994) show that increasing the G_{M1} content (range 0–30 mol % G_{M1}) of fluid chain EYPC/G_{M1} bilayers does lead to increased electron density in the interbilayer region, without significant change to the bilayer profile itself. Based on strip modeling studies, the increased interbilayer electron density is attributed to G_{M1} oligosaccharide occupying an 11–12 Å layer external to the egg PC bilayer surface. This effect is only weakly observed in the profile at 10 mol % G_{M1} (McIntosh and Simon, 1994), and at our lower G_{M1} content (5.7 mol %), specific location of the G_{M1} oligosaccharide is not possible (see above).

In summary, we have shown that ganglioside G_{M1} undergoes a broad transition which appears to be associated with a change in hydrocarbon chain packing in the micelle interior. In binary mixtures of G_{M1}/DPPC we have identified three zones in the temperature-composition phase diagram. In zone 1, up to ~30 mol % G_{M1} can be incorporated in DPPC bilayers both in the gel and liquid crystalline phases. In the gel phase, the main effect of G_{M1} (through its anionic sialic acid moiety) is to convert DPPC from a "limited-swelling" to an "infinite-swelling" lipid. At high concentrations (zone 3), G_{M1} forms mixed micelles containing DPPC which undergo similar broad phase transitions to G_{M1} itself. At intermediate concentrations (zone 2), bilayer disruption occurs and apparently two phases (bilayer and micellar/cylindrical) coexist.

We wish to thank Ms. Irene Miller for help in the preparation of the manuscript. This research was supported by research grant HL-26335 and training grant HL-07291 from the National Institutes of Health.

REFERENCES

Acquotti, D., L. Poppe, J. Dabrowski, C. von der Lieth, S. Sonnino, and G. Tettamanti. 1990. Three-dimensional structure of the oligosaccharide chain of GM1 ganglioside revealed by a distance-mapping procedure: a rotating and laboratory frame nuclear Overhauser enhancement investigation of native glycolipid in dimethyl sulfoxide and in water-dodecylphosphocholine. *J. Am. Chem. Soc.* 112:7772–7778.

Bach, D., I. R. Miller, and B. -A. Sela. 1982. Calorimetric studies on various gangliosides and ganglioside-lipid interactions. *Biochim. Biophys. Acta.* 686:233–239.

Brown, D., and J. K. Rose. 1992. Sorting of GPI-anchored proteins to glycolipid-enriched membrane subdomains during transport to the apical cell surface. *Cell.* 68:533–544.

Bunow, M. R., and B. Bunow. 1979. Phase behavior of ganglioside-lecithin bilayers. Relation to dispersion of gangliosides in membranes. *Biophys. J.* 27:325–337.

Cabral-Lilly, D., G. E. Sosinsky, R. A. Reed, M. R. McDermott, and G. G. Shipley. 1994. Orientation of cholera toxin bound to model membranes. *Biophys. J.* 66:935–941.

Cestaro, B., Y. Barenholz, and S. Gatt. 1980. Hydrolysis of di- and tri-sialo gangliosides in micellar and liposomal dispersion by bacterial neuraminidases. *Biochemistry.* 19:615–619.

Curatolo, W., D. M. Small, and G. G. Shipley. 1977. Phase behavior and structural characteristics of hydrated bovine brain gangliosides. *Biochim. Biophys. Acta.* 468:11–20.

Fishman, P. H., and R. O. Brady. 1976. Biosynthesis and function of gangliosides. *Science.* 194:906–915.

Fishman, P. H., T. Pacuszka, and P. A. Orlandi. 1993. Gangliosides as receptors for bacterial enterotoxins. *Adv. Lipid Res.* 25:165–187.

Fredman, P. 1993. Glycosphingolipid tumor antigens. *Adv. Lipid Res.* 25:213–234.

Gammack, D. B. 1963. Physical-chemical properties of ox-brain gangliosides. *Biochem. J.* 88:373–383.

Gillard, B. K., J. P. Heath, L. T. Thurmon, and D. M. Marcus. 1991. Association of glycosphingolipids with intermediate filaments of human umbilical vein endothelial cells. *Exp. Cell. Res.* 192:433–444.

Gulik-Krzywicki, T., A. Tardieu, and V. Luzzati. 1969. The smectic phase of lipid-water systems: properties related to the nature of the lipid and to the presence of net electrical charge. *Mol. Cryst. Liq. Cryst.* 8:285–291.

Haas, N. S., and G. G. Shipley. 1995. Structure and properties of *N*-palmitoleoyl galactosyl sphingosine (cerebroside). *Biochim. Biophys. Acta.* 1240:133–141.

Hakomori, S. I. 1981. Glycosphingolipids in cellular interaction, differentiation, and oncogenesis. *Annu. Rev. Biochem.* 50:733–764.

Hakomori, S. I. 1990. Bifunctional role of glycosphingolipids. Modulators for transmembrane signaling and mediators for cellular interactions. *J. Biol. Chem.* 265:18713–18716.

Hakomori, S. I., and Y. Igarashi. 1993. Gangliosides and glycosphingolipids as modulators of cell growth, adhesion, and transmembrane signaling. *Adv. Lipid Res.* 25:147–162.

Harris, P. L., and E. R. Thornton. 1978. Carbon-13 and proton magnetic resonance studies of gangliosides. *J. Am. Chem. Soc.* 100:6738–6745.

Higashi, H., A. Omori, and T. Yamagata. 1992. Calmodulin, a ganglia protein. Binding of gangliosides in the presence of calcium. *J. Biol. Chem.* 267:9831–9838.

Hill, M. W., and R. Lester. 1972. Mixtures of gangliosides and phosphatidylcholine in aqueous dispersions. *Biochim. Biophys. Acta.* 282:18–30.

Hinz, H. J., O. Korner, and C. Nicolau. 1981. Influence of gangliosides GM_1 and GD_{1a} on structural and thermotropic properties of sonicated small 1,2-dipalmitoyl-L-α-phosphatidylcholine vesicles. *Biochim. Biophys. Acta.* 643:557–571.

Hoekstra, D., and J. W. Kok. 1992. Trafficking of glycosphingolipids in eukaryotic cells: sorting and recycling of lipids. *Biochim. Biophys. Acta.* 1113:277–294.

Kihg, G. I. 1971. Low-angle x-ray diffraction studies of the nerve myelin sheath. Ph.D. thesis, University of Michigan. 107 pp.

King, G. I., and C. R. Worthington. 1971. Analytic continuation as a method of phase determination. *Physics Lett.* 35A:259–260.

Koerner, T. A. W. Jr., J. H. Prestegard, P. C. Demon, and R. K. Yu. 1983a. High-resolution proton NMR studies of gangliosides. 1. Use of homonuclear two-dimensional spin-echo J-correlated spectroscopy for determination of residue composition and anomeric configurations. *Biochemistry.* 22:2676–2687.

Koerner, T. A. W. Jr., J. H. Prestegard, P. C. Demon, and R. K. Yu. 1983b. High-resolution proton NMR studies of gangliosides. 2. Use of two-dimensional nuclear Overhauser effect spectroscopy and sialylation shifts for determination of oligosaccharide sequence and linkage sites. *Biochemistry.* 22:2687–2690.

Maggio, B., T. Ariga, J. M. Sturtevant, and R. A. Yu. 1985a. Thermotropic behavior of glycosphingolipids in aqueous dispersions. *Biochemistry.* 24:1084–1092.

Maggio, B., T. Ariga, J. M. Sturtevant, and R. A. Yu. 1985b. Thermotropic behavior of binary mixtures of dipalmitoylphosphatidylcholine and glycosphingolipids in aqueous dispersions. *Biochim. Biophys. Acta.* 818:1–12.

Maggio, B., F. A. Cumar, and R. Caputto. 1978a. Surface behavior of gangliosides and related glycosphingolipids. *Biochem. J.* 171:559–565.

Maggio, B., F. A. Cumar, and R. Caputto. 1978b. Interactions of gangliosides with phospholipids and glycosphingolipids in mixed monolayers. *Biochem. J.* 175:1113–1118.

Maggio, B., F. A. Cumar, and R. Caputto. 1980. Configuration and interaction of the polar head group in gangliosides. *Biochem. J.* 189: 435–440.

Maggio, B., F. A. Cumar, and R. Caputto. 1981. Molecular behavior of glycosphingolipids in interfaces. Possible participation in some properties of nerve membranes. *Biochim. Biophys. Acta.* 650:69–87.

Maggio, B., G. G. Montich, and F. A. Cumar. 1988. Surface topography of sulfatide and gangliosides in unilamellar vesicles of dipalmitoylphosphatidylcholine. *Chem. Phys. Lipids.* 46:137–146.

Masserini, M., and E. Freire. 1986. Thermotropic characterization of phosphatidylcholine vesicles containing ganglioside GM1 with homogeneous ceramide chain length. *Biochemistry.* 25:1043–1049.

McDaniel, R. V., and T. J. McIntosh. 1986. X-ray diffraction studies of the cholera toxin receptor, G_{M1}. *Biophys. J.* 49:94–96.

McIntosh, T. J., and S. A. Simon. 1986. Hydration force and bilayer deformation: a reevaluation. *Biochemistry.* 25:4058–4066.

McIntosh, T. J., and S. A. Simon. 1994. Long- and short-range interactions between phospholipid/ganglioside GM1 bilayers. *Biochemistry.* 33: 10477–10486.

Mehlhorn, I. E., G. Parraga, K. R. Barber, and C. W. M. Grant. 1986. Visualization of domains in rigid ganglioside/phosphatidylcholine bilayers: Ca^{2+} effects. *Biochim. Biophys. Acta.* 863:139–155.

Myers, M., C. Wortman, and E. Freire. 1984. Modulation of neuraminidase activity by the physical state of phospholipid bilayers containing gangliosides G_{d1a} and G_{t1b}. *Biochemistry.* 23:1442–1448.

Norton, W. T., and S. E. Poduslo. 1971. Neuronal perikarya and astroglia of rat brain: chemical composition during myelination. *J. Lipid Res.* 12:84–90.

Parton, R. G., and Simons, K. 1995. Digging into caveolae. *Science.* 269:1398–1399.

Perillo, M. A., A. Polo, A. Guidotti, E. Costa, and B. Maggio. 1993. Molecular parameters of semisynthetic derivatives of gangliosides and sphingosine in monolayers at the air-water interface. *Chem. Phys. Lipids.* 65:225–238.

Peters, M. W., I. E. Mehlhorn, K. R. Barber, and C. W. M. Grant. 1984. Evidence of a distribution difference between two gangliosides in bilayer membranes. *Biochim. Biophys. Acta.* 778:419–428.

Reed, R. A., and G. G. Shipley. 1987. Structure and metastability of *N*-lignoceryl galactosylsphingosine (cerebroside) bilayers. *Biochim. Biophys. Acta.* 896:153–164.

Reed, R. A., and G. G. Shipley. 1988. Effect of chain unsaturation on the structure and thermotropic properties of galactosyl cerebrosides. *Biophys. J.* 55:281–292.

Reed, R. A., J. M. Mattai, and G. G. Shipley. 1987. Interaction of cholera toxin with ganglioside G_{M1} receptors in supported lipid monolayers. *Biochemistry.* 26:824–832.

Ruocco, M. J., D. Atkinson, D. M. Small, R. Skarjune, E. Oldfield, and G. G. Shipley. 1981. X-ray diffraction and calorimetric study of anhydrous and hydrated *N*-palmitoylgalactosylsphingosine (cerebroside). *Biochemistry.* 20:5957–5966.

Ruocco, M. J., E. Oldfield, and G. G. Shipley. 1983. Galactocerebroside-phospholipid interactions in bilayer membranes. *Biophys. J.* 43:91–101.

Ruocco, M. J., and G. G. Shipley. 1984. Interaction of cholesterol with galactocerebroside and galactocerebroside-phosphatidylcholine bilayer membranes. *Biophys. J.* 46:695–707.

Ruocco, M. J., and G. G. Shipley. 1986. Thermal and structural behavior of natural cerebroside-3-sulfate in bilayer membranes. *Biochim. Biophys. Acta.* 859:246–256.

Sabesan, S., K. Bock, and R. U. Lemieux. 1984. The conformational properties of the gangliosides GM2 and GM1 based on ^1H and ^{13}C nuclear magnetic resonance studies. *Can. J. Chem.* 62:1034–1035.

Sabesan, S., J. O. Duus, T. Fukunaga, K. Bock, and S. Ludvigsen. 1991. NMR and conformational analysis of ganglioside GD1a. *J. Am. Chem. Soc.* 113:3326–3246.

Sayre, D. 1952. Some implications of a theorem due to Shannon. *Acta Crystallogr.* 5:843.

Scarsdale, J. N., J. H. Prestegard, and R. K. Yu. 1990. NMR and computational studies of interactions between remote residues in gangliosides. *Biochemistry.* 29:9843–9855.

Schnitzer, J. E., D. P. McIntosh, A. M. Dvorak, J. Liu, and P. Oh. 1995. Separation of caveolae from associated microdomains of GPI-anchored proteins. *Science.* 269:1435–1439.

Shannon, C. E. 1949. Communication in the presence of noise. *Proc. Inst. Radio Eng. NY.* 37:10–21.

Siebert, H.-C., G. Reuter, R. Schauer, C.-W. von der Lieth, and J. Dabrowski. 1992. Solution conformations of GM3 gangliosides containing different sialic acid residues as revealed by NOE-based distance mapping, molecular mechanics, and molecular dynamics calculations. *Biochemistry.* 31:6962–6971.

Sillerud, L. O., D. E. Schafer, R. K. Yu, and W. H. Konigsberg. 1979. Calorimetric properties of mixtures of ganglioside G_{M1} and dipalmitoylphosphatidylcholine. *J. Biol. Chem.* 254:10876–10880.

Singh, D., H. C. Jarrell, K. R. Barber, and C. W. M. Grant. 1992. Glycosphingolipids: ^2H NMR study of the influence of ceramide fatty acid characteristics on the carbohydrate headgroup in phospholipid bilayers. *Biochemistry.* 31:2662–2669.

Svennerholm, L., and P. Fredman. 1980. A procedure for the quantitative isolation of brain gangliosides. *Biochim. Biophys. Acta.* 617:97–109.

Tettamanti, G., and L. Riboni. 1993. Gangliosides and modulation of the function of neural cells. *Adv. Lipid Res.* 25:235–267.

Thompson, T. E., M. Allieta, R. E. Brown, M. L. Johnson, and T. W. Tillack. 1985. Organization of ganglioside G_{M1} in phosphatidylcholine bilayers. *Biochim. Biophys. Acta.* 817:229–237.

Torbet, J., and M. H. F. Wilkins. 1976. X-ray diffraction study of lecithin bilayers. *J. Theor. Biol.* 62:447–458.

Worthington, C. R., and A. E. Blaurock. 1969. A structural analysis of nerve myelin. *Biophys. J.* 9:970–990.

Zeller, C. B., and R. B. Marchase. 1992. Gangliosides as modulators of cell function. *Am. J. Physiol.* 262:C1341–C1355.

Zhang, R., D. L. Scott, M. L. Westbrook, S. Nance, B. D. Spangler, G. G. Shipley, and E. M. Westbrook. 1995b. The three-dimensional crystal structure of cholera toxin. *J. Mol. Biol.* 251:563–573.

Zhang, R., M. L. Westbrook, E. M. Westbrook, D. L. Scott, Z. Otwinowski, P. R. Maulik, R. A. Reed, and G. G. Shipley. 1995a. The 2.4 crystal structure of cholera toxin B subunit pentamer: choleragenoid. *J. Mol. Biol.* 251:550–562.